Multi-layered Spectral Formation in SNe Ia Around Maximum Light

Sebastien Bongard[1,2,4], E. Baron[2,3], G. Smadja[4], David Branch[2], and Peter H. Hauschildt[5]

ABSTRACT

We use the radiative transfer code PHOENIX to study the line formation of the wavelength region 5000–7000 Å. This is the region where the SNe Ia defining Si II feature occurs. This region is important since the ratio of the two nearby silicon lines has been shown to correlate with the absolute blue magnitude. We use a grid of LTE synthetic spectral models to investigate the formation of line features in the spectra of SNe Ia. By isolating the main contributors to the spectral formation we show that the ions that drive the spectral ratio are Fe III, Fe II, Si II and S II. While the first two strongly dominate the flux transfer, the latter two form in the same physical region inside of the supernova. We also show that the naïve blackbody that one would derive from a fit to the observed spectrum is far different than the true underlying continuum.

Subject headings: cosmology — stars: atmospheres — supernovae

DISCLAIMER

[1]Physics Division, Lawrence Berkeley National Laboratory, MS 50A-5014, 1 Cyclotron Rd, Berkeley, CA 94720-8139 USA; email: sbongard@lbl.gov

[2]Homer L. Dodge Department of Physics and Astronomy, University of Oklahoma, 440 West Brooks, Rm. 100, Norman, OK 73019, USA; email: baron@ou.edu, branch@nhn.ou.edu

[3]Computational Research Division, Lawrence Berkeley National Laboratory, MS 50F-1650, 1 Cyclotron Rd, Berkeley, CA 94720-8139 USA

[4]Institut de Physique Nucléaire Lyon, Bâtiment Paul Dirac Université Claude Bernard Lyon-1 Domaine scientifique de la Doua 4, rue Enrico Fermi 69622 Villeurbanne cedex, France; email: smadja@in2p3.fr

[5]Hamburger Sternwarte, Gojenbergsweg 112, 21029 Hamburg, Germany; email: yeti@hs.uni-hamburg.de

1. Introduction

Type Ia supernovæ have been used as "standardizable candles" for more than 10 years, thanks to the correlation between their light curve shape and their absolute blue magnitude at maximum light. This correlation is well matched by a spectroscopic sequence (Nugent et al. 1995) defined by the ratio, $\Re_{Si}$, of the depth of two absorption features usually identified as Si II λ5972 and λ6355 lines. Using the radiative transfer code `PHOENIX` (Hauschildt & Baron 1999; Baron & Hauschildt 1998; Hauschildt et al. 1997a,b, 1996, and references therein), this sequence has been matched to a temperature sequence that could physically be related to the amount of ^{56}Ni produced in the context of Chandrasekhar-mass white dwarf explosions.

Hatano et al. (2000) showed that $\Re_{Si}$ and the velocity derived from the minimum of the $\approx$ 6100 Å feature correlated poorly, suggesting that a one-parameter description of SNe Ia was insufficient. This velocity derived from the P-Cygni feature associated with the Si II λ6355 line, and its time evolution break SNe Ia into subclasses depending upon more than one parameter (Benetti et al. 2005). Branch et al. (2006) and Hachinger et al. (2006) also showed that different spectroscopic indicators exist which can be used to distinguish variations even within the "normal" SNe Ia. In the context of Chandrasekhar-mass explosions, these variations cannot be interpreted only in terms of differences in the amount of ^{56}Ni produced. The velocity scatter could be due to properties of the progenitor system that impact on the kinetic energy released during the explosion. For example, the ratio (^{54}Fe+^{58}Ni)/^{56}Ni has been proposed as a second physical parameter which could account for this dispersion (Mazzali & Podsiadlowski 2006).

This paper is an attempt to unravel the spectral formation in the $5000 - 7000$ Åregion (henceforth the $\Re_{Si}$ wavelength region), as a way to address the physical reasons for their correlation with luminosity, and especially the link between this correlation and the temperature sequence of SNe Ia. A previous attempt using the radiative transfer code SYNOW

(Fisher 2000), was performed by Garnavich et al. (2004) who explained the counter-intuitive correlation of $\Re_{Si}$ with luminosity by the temperature sensitivity of a Ti II line. On the other hand synthetic spectral investigations (Stehle et al. 2005; Branch et al. 2006) failed to find any important Ti II line contributions in this part of the spectrum.

We use the radiative transfer code PHOENIX differently than it has usually been used previously. Instead of fitting a supernova by varying the time and bolometric luminosity, we use a grid of simulated models to probe the line formation process. Our input model is the parametrized deflagration model W7 (Nomoto et al. 1984), homologously expanded to calculate the abundances at any given time. The knowledge of the abundance structure of the explosion model, and the self-consistent physical structure provided by PHOENIX are used to describe more precisely how the spectrum is formed in SNe Ia. Bongard et al. (2006) introduced the line ratio $\Re_{SiS}$, which is defined as the ratio of two integrals of the flux over a chosen wavelength range, where each integral is centered around the two lines used in the original definition of $\Re_{Si}$ (see §6.1). It is designed to be useful for spectra which have lower signal to noise than well-observed nearby SNe Ia.

This understanding of the formation of the spectrum allows us to explain why the line ratio $\Re_{SiS}$ is a good probe of the temperature sequence, and reinforces the link between this sequence and the absolute blue magnitude of SNe Ia. These results also allow us to rule out a Ti II contribution to the correlation of $\Re_{Si}$ with luminosity. We emphasize that even though the synthetic spectra presented here *do not* do a good job of reproducing observed SNe Ia spectra, we consider W7 to be the fiducial SNe Ia model. Baron et al. (2006) showed that reasonably good synthetic spectra can be produced with W7 near maximum light. We make differential comparisons based on that model, keeping in mind that Baron et al. (2006) emphasized that W7 did not reproduce the wavelength region that we examine in detail here.

We will address time evolution only qualitatively. The goal of this paper is to understand the temperature sequence of SNe Ia spectra around maximum light, thus we concentrated on day 20 after explosion, since maximum light in B in SNe Ia has been shown to occur 18–25 days after explosion.

2. Analysis tool: PHOENIX simulations

2.1. The LTE grid

Using the multi-purpose radiative transfer code PHOENIX we converged LTE calculations for the W7 explosion model at 10, 15, 20, and 25 days after explosion, for a range of bolometric luminosities spanning the "normal" supernovæ blue magnitudes.

2.2. Single Ion spectra

Each model converged with PHOENIX not only provides a spectrum, but also the knowledge of the physical structure and line optical depth in the supernova. This gives us the ability to compute "single ion spectra" as follows: Using the converged output of the PHOENIX simulation, we artificially turn off all but the continuum and one single ion line opacities. The "continuum opacities" denote all the bound-free and free-free opacities as well as electron and Rayleigh scattering. We then recalculate the solution of the scattering problem in order to get the "single ion spectrum", with the level populations and free electron number kept fixed.

The relative strength of the absorption and emission features in this spectrum give an indication of the contribution of each line to the complete spectrum. Since the solution of the scattering problem is recalculated, the features are *not* expected to look exactly the same as in the complete spectrum. In any case, due to the global nature of the transfer equation, the full spectrum in *not* the linear combination of all the single ion spectra.

In these single ion spectra, the flux transfer from the blue to the red due to scattering will be smaller, due to the opacity decrease caused by the suppression of most of the ions. They will thus appear bluer than the complete spectrum. The back scattering will also be decreased for the same reason, resulting in "single ion spectra" brighter than the full synthetic spectrum.

The ratio of scattering to absorption is larger in the single ion spectra compared to the full synthetic spectrum because the full scattering problem is solved with fixed level populations and fewer atomic lines. The same effect enhances stimulated emission in the single ion spectra, resulting in strong net emission in the P-Cygni profiles.

Since the single ion spectra are always brighter than the full synthetic spectrum we must normalize the luminosity in order to compare the two spectra. We do this by setting the single ion bolometric luminosity to that of the full synthetic spectrum. This procedure is trivial since the synthetic spectra include fluxes at all wavelengths.

The special case we name "continuum-only spectrum" is that where all line opacities are set to zero, and therefore the spectrum is due to pure continuum processes. In a moving atmosphere a photoionization edge can produce a feature that looks like a P-Cygni line (Baron et al. 1999). We can turn on and off different species individually, thus we can, for example, have a "two-ion" spectrum that consists of, for example, only Si II and S II.

3. Using single ion spectra: ruling out a Ti II contribution to $\Re_{Si}$

3.1. The $\Re_{Si}$ puzzle

Because of their similar redshift with respect to Si II λ6355 and Si II λ5972 lines it is tempting to consider the 6100 Å and 5800 Å troughs to be part of their P-Cygni profiles. These two lines share the 4P level, the λ6355 line is the 4S-4P transition and the λ5972 is the 4P-5S transition. Their optical depths can thus be estimated in the Sobolev approximation using (Hatano et al. 1999):

$$\tau = (\frac{\pi e^2}{mc}) f \, \lambda \, t \, n_l \, [1 - \frac{g_l n_u}{g_u n_l}], \tag{1}$$

where n_l and n_u are the number densities of the lower and upper level associated with the transition, f is its oscillator strength, t is the time since explosion, g_l and g_u are the statistical weights of the levels, and λ is the wavelength of the transition. Assuming thermal equilibrium, the ratio of the Si II λ6355 line optical depth (τ_{red}) over the Si II λ5972 line optical depth (τ_{blue}) becomes:

$$\frac{\tau_{red}}{\tau_{blue}} \propto \frac{\frac{1}{3} \, e^{\Delta_{E_{red}}/(k_B T)} - 1}{1 - 3 \, e^{-\Delta_{E_{blue}}/(k_B T)}} \tag{2}$$

where ΔE is the energy difference between the upper and lower levels of the transition. This ratio decreases monotonically with respect to a temperature increase, as also shown in Fig. 1, where SYNOW was used to compute Si II spectra for excitation temperatures ranging from 5000 K to 40000 K.

Since P-Cygni troughs become deeper with increasing optical depth, a higher Si II excitation temperature should increase $\Re_{Si}$. Under the reasonable assumption that higher luminosity SNe Ia have higher Si II excitation temperatures, $\Re_{Si}$ should increase and not decrease with luminosity. Observations show the opposite behavior.

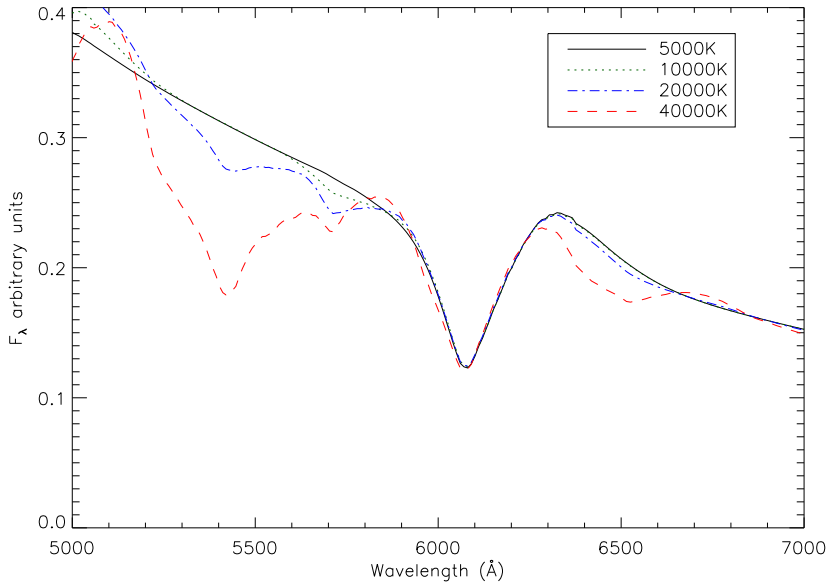

Fig. 1.— Si II in SYNOW for increasing excitation temperatures. The trough of the blue feature due to Si II λ5972 increases relative to the trough of the Si II λ6355 feature as temperature increases, as predicted by Eq. 2. The Si II reference line is Si II λ6355 and only the excitation temperature is varied, which explains the $\sim$ 6100 Å trough stability. (Note that the unrealistic excitation temperature of 40000K leads to a very strong feature around 5400 Å that is not observed in SNe Ia spectra.)

Fig. 2 displays the temperature structure from our grid of calculations 20 days after explosion with increasing bolometric luminosities. We restricted the plot to the $9000 - 16000$ km s^{-1} region, where silicon is found in W7. This shows the physical temperature increases with bolometric luminosity as one would expect. In LTE, a temperature increase results in a Si II excitation temperature increase with luminosity which would lead to an $\Re_{Si}$ increase with luminosity. Therefore, unless one assumes a temperature structure inversion in the $9000 - 16000$ km s^{-1} region due to NLTE effects, Si II lines alone are unable to explain the trend of the $\Re_{Si}$ correlation with SNe Ia blue magnitude.

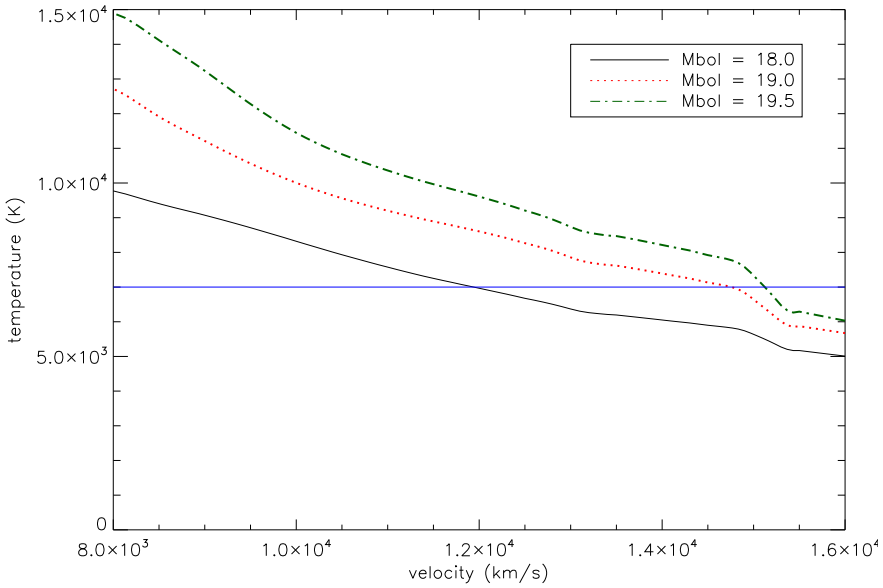

Fig. 2.— Temperature for day 20 models in the 8000-16000 km s^{-1} region where Si II ions are found, as a function of the model parameter M_{bol}. The horizontal blue line marks the 7000 K limit at which Ti II lines have been suggested to dominate over Si II λ5972 (Garnavich et al. 2004).

3.2. Ti II impact on the "$\Re_{Si}$ wavelength region"

Garnavich et al. (2004) proposed that $\Re_{Si}$ variation with luminosity could be accounted for by a blend of Ti II lines. We focus on the behavior of the λ6013 line. Garnavich et al. (2004) suggested that the the $\Re_{Si}$puzzle, described above could be solved by the temperature evolution of this line, which increases much faster than the Si II λ5972 line decreases below 7000 K.

In order to probe this assumption we display in Fig. 3 the day 20 two-ion spectra of Si II and Ti II alone as well as the full spectrum for our lower luminosity model. We also display the continuum-only spectrum as a reference. For Si II, the 6100 Å trough and the concomitant emission peak are, as expected, dominated by Si II lines, but the Si II λ5972 P-Cygni profile lacks the full spectrum blue edge, hinting at a missing contribution to the full spectrum line profile. This other contribution can not be Ti II as no Ti II lines appear in the $\Re_{Si}$ wavelength region, even though the Ti II λ6013 line has been checked to form between 12000 and 16000 km s^{-1}, where the temperature is below 7000 K as indicated by the black line in Fig. 2.

One could argue that this line does not appear in our two-ion spectrum because of a too low abundance of titanium in W7. We rule out the low abundance in W7 as an explanation for this effect since the Ti II single ion spectrum shows a strong feature to the blue of 5000 Å, which does a reasonably good job of reproducing the observed trough seen in fast decliner SNe Ia such as SN 1991bg.

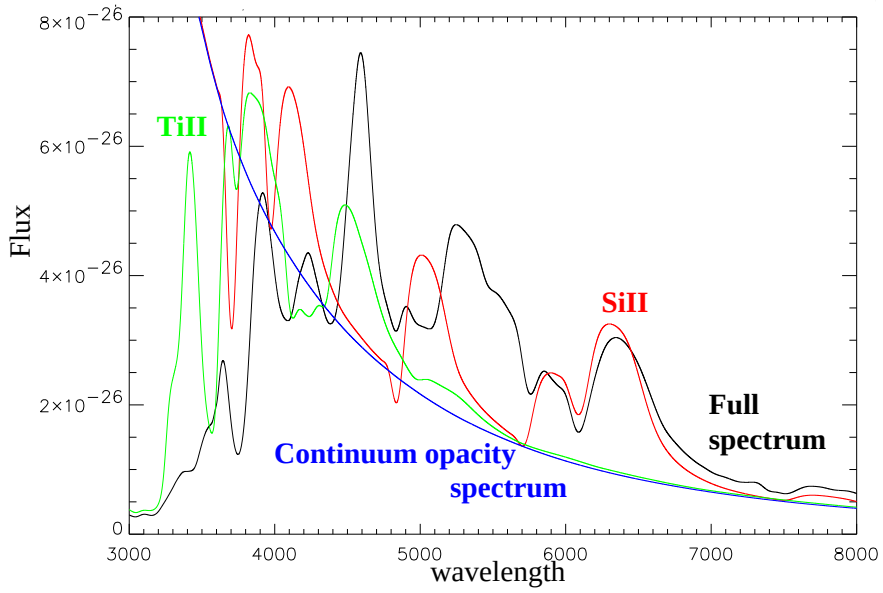

Fig. 3.— The single ion day 20 spectrum of Si II and Ti II alone as well as the full spectrum for our lower luminosity model. We also display the continuum-only spectrum as a reference.

Fig. 2 shows the PHOENIX temperature structure between 10000 and 16000 km s^{-1}, where the Si II and Ti II lines of the $\Re_{Si}$ wavelength region form in all our synthetic spectra models. Using SYNOW we were able to fit the $\Re_{Si}$ wavelength region with Si II and Ti II lines alone, but required a Ti II excitation temperature of 40000 K. This temperature is way too high compared to the detailed PHOENIX results, but note that the temperature in SYNOW is dependent on the chosen reference line. However, even with SYNOW, one expects that Ti II line strength increases with *decreasing* temperature. What is happening in this case, is that in order to obtain a noticeable contribution of Ti II (with respect to Si II), we must go to very high excitation temperatures combined with extremely large optical depths in Ti II: the temperature dependence is not independent of the Ti II optical depth, which in SYNOW is a free parameter.

This very high excitation temperature does not necessarily indicate that the assumptions of SYNOW have broken down, since the PHOENIX and SYNOW Ti II spectra agree quite well for similar temperatures. In Fig. 4 we display the comparison between the SYNOW results and the PHOENIX results in the temperature range appropriate to the physical results from PHOENIX. The Si II and the Ti II line strengths agree. We also agree with the point of Garnavich et al. (2004) that the temperature dependence of the strength of Ti II is such that the line-strength increases dramatically below 7000 K; however, the relative strength of the line with respect to Si II does not increase fast enough for the Ti II line to become important at reasonable physical temperatures. This is due to the fact that the initial line strength of Ti II is so small.

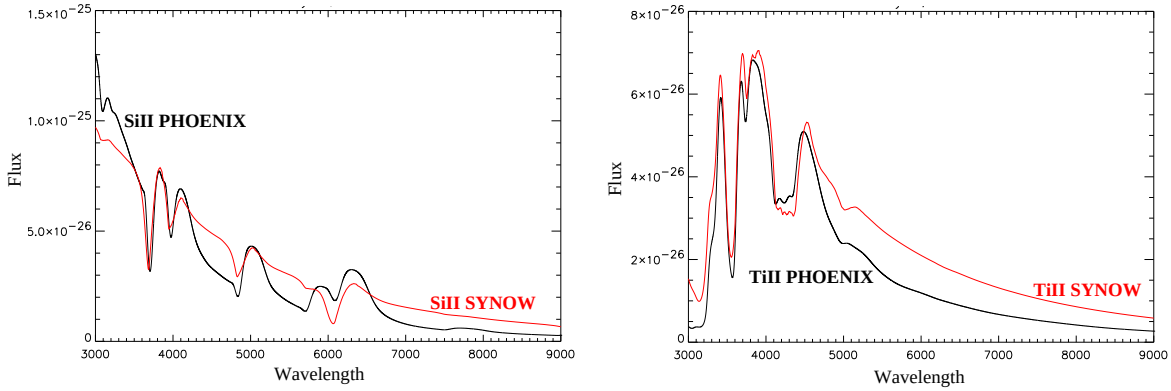

Fig. 4.— SYNOW and PHOENIX single ion spectra with SYNOW excitation temperature matching PHOENIX temperature structure. Left panel: Si II, right panel Ti II.

4. Multi-layered spectrum formation

4.1. The deepest layer

The multi-layer spectrum formation picture alters the way that one thinks about how spectrum formation occurs. In the photospheric picture, one thinks about features forming in a reversing layer, above a true continuum. In the multi-layer picture, features can form throughout the supernova atmosphere and can in principle imprint a shape into the "continuum" that is altered higher up in the atmosphere. The most important difference between the multi-layer picture and the photospheric picture is that features from multiple ionization stages can strongly affect the overall spectrum.

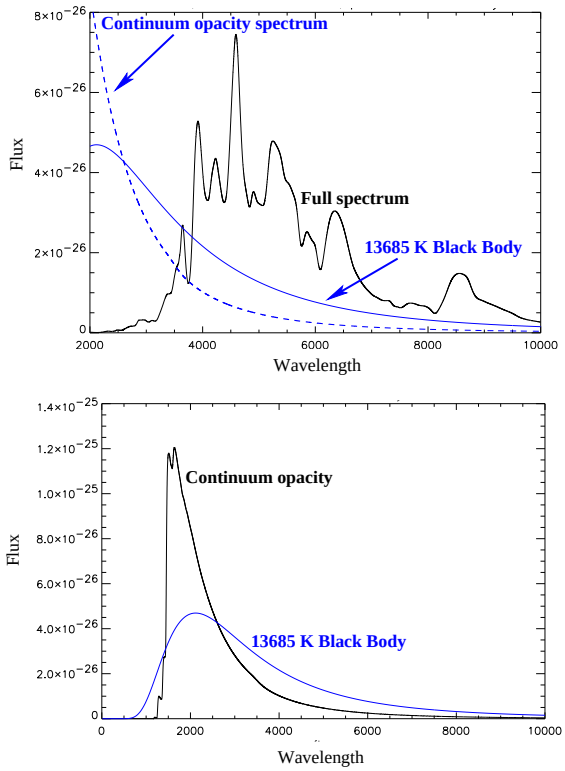

Fig. 5.— The naïve blackbody fit would peak where the full synthetic spectrum does, that is around 5000 Å, far to the red of the physical blackbody. Top Panel: Full PHOENIX day 20 spectrum in black, continuum-only spectrum forming below 2000 km s^{-1} in dotted blue, $13685K$ blackbody in plain blue. Bottom Panel: Continuum-only day 20 spectrum in dotted blue, and $13685K$ blackbody in plain blue.

In Fig. 5 (top panel) we display the deepest layer of the spectral formation of our lower bolometric luminosity model: the continuum-only spectrum. It forms below 3000 km s^{-1} for all our range of bolometric luminosities, where the continuum optical depth becomes greater than one, which is at a much lower velocity than where the photosphere is usually considered to be in the photospheric model.

Figure 5 (bottom panel) clearly shows that the naïve blackbody fit (that is the blackbody which peaks at the same wavelength as the smoothed full synthetic spectrum) to the full synthetic spectrum would give a blackbody temperature that is much cooler than the true underlying continuum. While the continuum-only spectrum is brighter and bluer (as described in §2.2) Fig. 5 (bottom panel) shows that the blackbody obtained from the physical temperature 13685 K is also significantly bluer than the naïve blackbody. This is a very important point since it shows that the naïve blackbody has nothing to do with the real physical conditions.

It is crucial to keep this point in mind when analyzing SNe Ia features, especially when using techniques like principle component analysis (PCA, James et al. 2006). It is tempting to subtract a "continuum" case by case in order to maximize the contribution of the lines. Since the "pseudo-continuum" is responsible for a large part of the spectral structure, this procedure yields the opposite result: the subtracted "continuum" adds a fake relationship between features. The PCA eigenvectors will thus no longer account only for real SNe Ia diversity, but also for the arbitrary continuum.

The blackbody of Fig. 5 (bottom panel) corresponds to the temperature where $\tau_e \sim 1$. Even at depth of 2000 km s^{-1} ($\tau \sim 3$ at 2000 km s^{-1}), the supernova spectrum is *not* a blackbody spectrum. The spectrum of the full W7 model is obtained from the steep narrow blue continuum-only spectrum by line interactions that transfer flux toward the red by Doppler shift or fluorescence.

4.2. Iron lines

In Fig. 6 we display the Fe II, Fe III and Fe II+Fe III two-ion spectra of our faintest model at day 20. The $\Re_{Si}$ wavelength region ($5000 - 7000$ Å) gives us some insight into the spectral formation process because of the smaller number of strong lines than in the bluer spectral regions. The Fe III and the Fe II peaks at 5900 Å and 6100 Å are blends of weak lines formed at velocities of $\sim$ 5000 and $\sim$ 9000 km s^{-1}, respectively. It follows from the optical depths shown in Fig. 11 that the 5128 Å Fe III peak and the 5170 Å Fe II peak arise from strong lines formed at velocities of $\sim$ 7000 and $\sim$ 15000 km s^{-1}, respectively.

Fig. 6 shows how Fe III and Fe II lines blend together. The strong Fe III 5128 Å feature is shielded by the strong Fe II 5170 Å one, and the two blends above 5900 Å merge together.

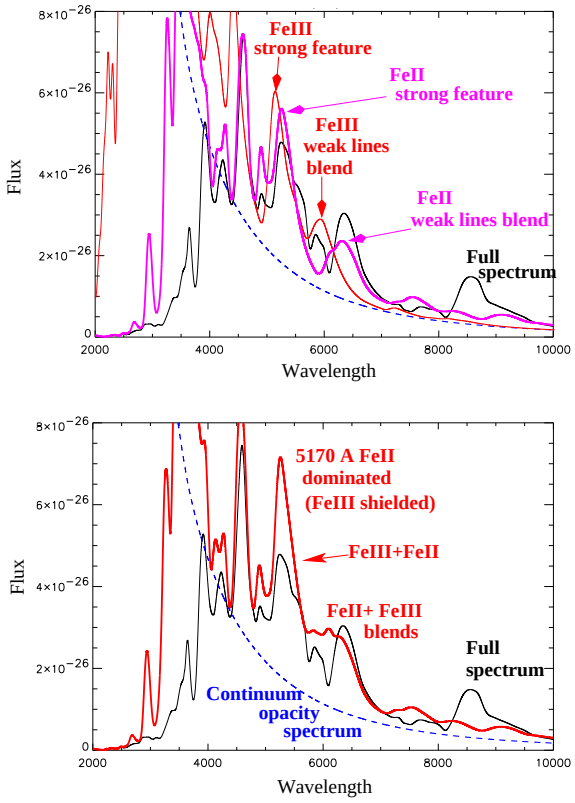

Fig. 6.— Fe II and Fe III single ion spectra for our faintest simulated spectra, 20 days after explosion. The top panel is Fe III in red and Fe II in pink. The bottom panel is Fe II + Fe III two-ion spectra in red. In both cases the black spectrum is the full simulated spectrum and the blue spectrum is the continuum-only spectrum.

In the photospheric model the spectrum is considered to be a blackbody continuum emitted by the photosphere on top of which strong, well-separated lines of ions present in the line forming region add structure mainly by scattering light. We define the "pseudo-continuum" as the spectrum formed by weak line blends which produces more structure than a blackbody spectrum. The photosphere is replaced in this picture by a "pseudo-photosphere" forming at depth depending on wavelength. This concept is widely used in the radiative transfer community.

This "pseudo-photosphere" is clearly seen in the results of Branch et al. (2005) who were able to model the spectrum of the normal SN Ia 1994D using SYNOW at 115 days past maximum light, at least in the blue. Specifically, the results of Branch et al. (2005) show that even at late times (thus in the deepest layers) the spectrum is dominated by permitted lines that can be treated in resonant scattering.

Similarly, the line forming region of the pseudo-photospheric model does not have a fixed depth. We define it as the region where the strong lines that create the final structure of the spectrum form. In this picture, the strong Fe III 5128 Å feature does not belong to the line forming region because it forms in the same physical region as the weak Fe II lines of the pseudo-photosphere with which it blends, as can be seen in Fig. 11. It adds structure to the pseudo-continuum and is shielded by the strong Fe II 5170 Å feature forming further out. The existence of strong lines that form deep and of weaker lines that imprint their features further out in the atmosphere leads to a convergence between the pseudo-photospheric region and the line forming region, making it almost impossible to separate them into two clearly distinct physical regions.

The Fe II+Fe III spectrum we display in Fig. 6 can be considered to be the pseudo-continuum spectrum in the $5000 - 7000$ Å region. It is formed by a large peak due to Fe III λ5128 and neighboring strong Fe II lines, followed by a flat region forming between 5000 and 9000 km s^{-1} depending on wavelength. This shows that by construction $\Re_{Si}$ couples spectral regions that form at very different depths.

In the "pseudo-photospheric" model, the flux transfer from the blue toward the red is dominated by Fe III and Fe II weak line blends. Of course, weak cobalt and nickel lines also contribute, but the study of their effects will be postponed to a later paper in which the more complicated spectral formation in the $\lambda < 5000$ Å region will be discussed. The colors of SNe Ia are therefore dominated by weak lines of the heavy elements whose blending shapes the pseudo-photosphere spectrum.

5. Iron lines and colors

As the bolometric luminosity of our models is increased, the temperature also rises, ionizing Fe II to Fe III. The Fe II number abundance depletion decreases the 5170 Å feature strength, leaving S II the dominant ion of the blue edge of the $\Re_{Si}$ feature at $\sim$ 5455 Å. This effect can be seen in Figs. 8–10 where the Fe III, Fe II, Si II, and S II spectrum changes with bolometric luminosity are displayed. The Fe II 5170 Å feature strength decreases as Fe II is ionized into Fe III, unshielding the strong Fe III 5128 Å feature. Simultaneously, the flux transfer towards the red decreases because Fe II is much more efficient at transferring flux toward the red than Fe III as can be seen in Fig. 6. This efficient flux transfer from the blue to the red is due to numerous blue and UV Fe II lines that amount to a large opacity because of line blanketing.

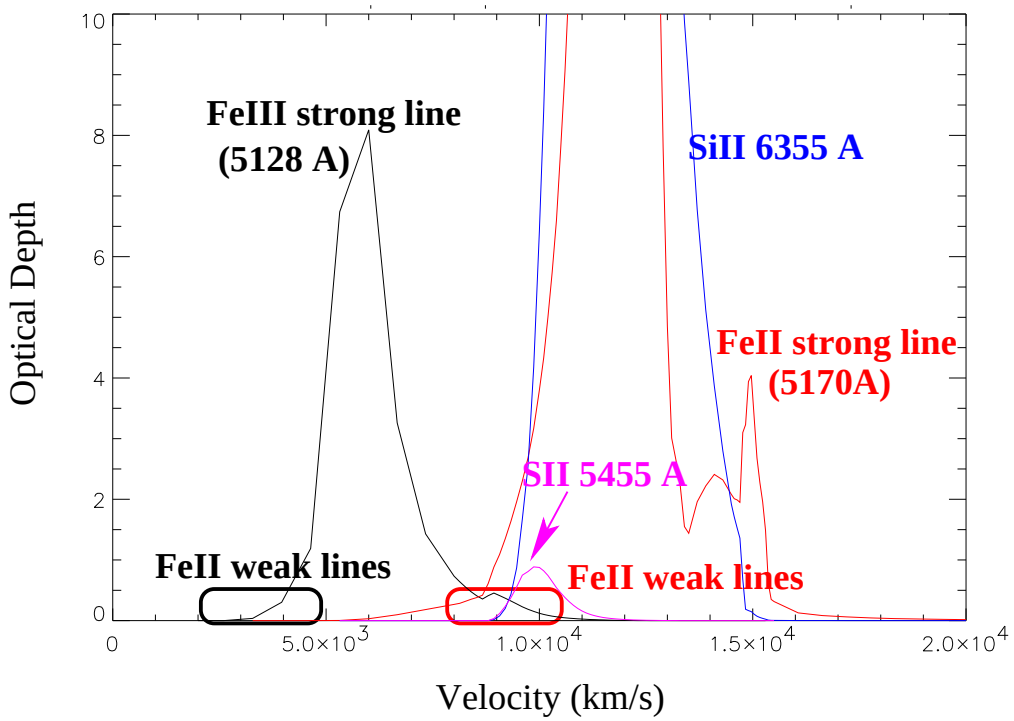

Fig. 7.— $B-V$ color as a function of M_{bol} for the different epochs in our grid.

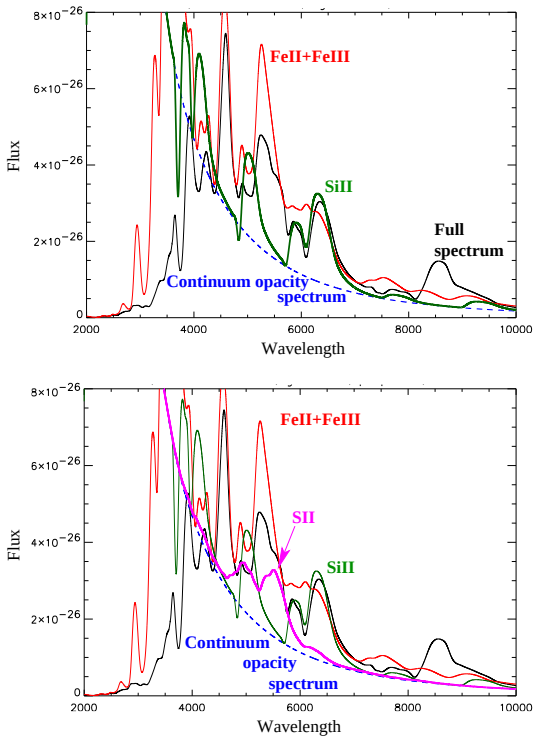

Fig. 8.— Fe II (top panel) and Fe III (bottom panel) day 20 single ion spectra as a function of M_{bol}. Each spectrum is rescaled to the bolometric flux of the corresponding full synthetic spectrum. Since Fe III forms deeper it is less sensitive to a change in the bolometric luminosity. Fe II lines are more efficient at transferring flux from blue to red.

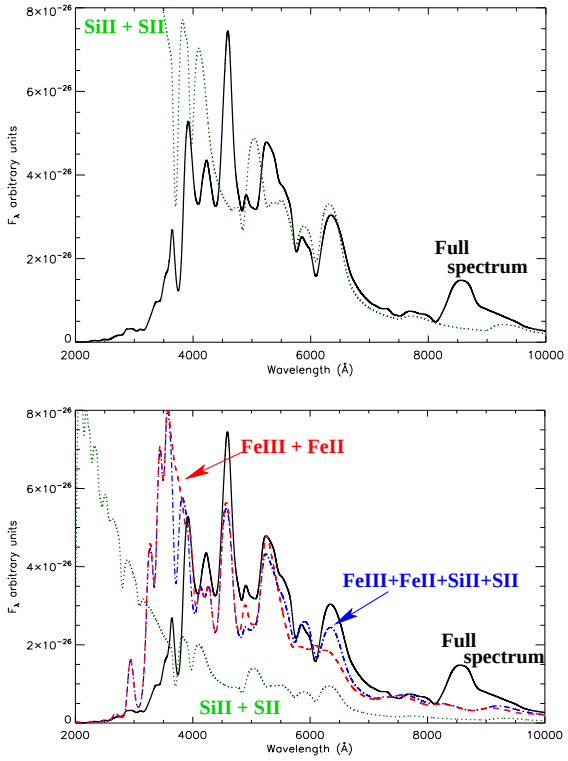

Fig. 9.— Fe II + Fe III (top panel) and Si II + S II (bottom panel) two-ion day 20 spectra as a function of M_{bol}. The flux transfer from the blue to the red is dominated by the iron (and other iron peak elements in the full spectrum). All spectra are rescaled to have the same flux as the corresponding full synthetic spectra.

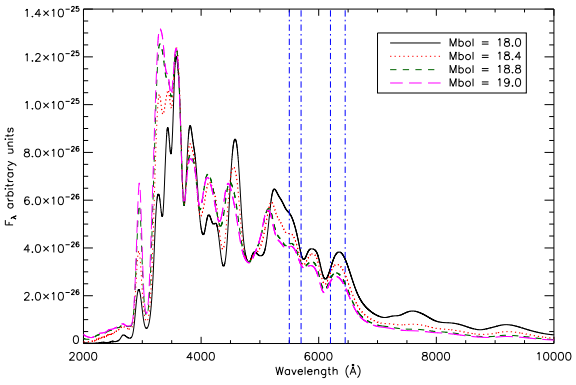

Fig. 10.— Fe III+Fe II+Si II+S II four-ion day 20 spectra as a function of M_{bol}.

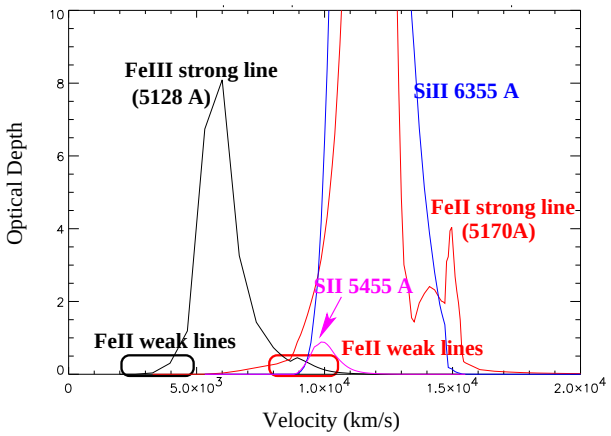

Fig. 11.— Optical depth of the most important lines of the $\Re_{Si}$ wavelength region at day 20. Weak lines always form deeper than the strong ones for Fe II and Fe III. Fe III λ5128 and Fe II λ 5170 are displayed as typical examples of strong Fe III and Fe II lines in the $\Re_{Si}$ wavelength region.

Figure 6 also shows that in the 5000-8000 Å wavelength region, Fe III features remain very stable over the range of bolometric luminosities explored, while Fe II features vary much more. This is not surprising, as Fe III lines form much deeper, in a region that is hotter and denser, where physical conditions vary less than in the outer regions.

We see in Figure 9 (top panel) that the Fe III+Fe II two-ion spectrum undergoes a strong increase of flux below 5500 Å, while it remains very stable above, when the bolometric luminosity increases. This translates into a strong variation in color of the full synthetic spectrum. On the other hand, the Si II+S II two-ion spectra displayed in Fig. 9 (bottom panel) remain very consistent in shape, while their flux follows the continuum-only spectrum flux increase.

The flux variation displayed in Fig. 10 is thus dominated by the "pseudo-continuum" of Fe III and Fe II lines, especially the weak line blends, on top of which the strong Si II and S II lines add structure. The flux transferred by the well separated lines formed in the line forming region is small compared to the flux transferred at depth by iron lines, but is by no means negligible when using SNe Ia for precision cosmology. It is therefore crucial to have a good description of the full spectrum in order to perform K-corrections.

Figure 14 shows very close agreement between the full synthetic spectrum and the Fe III+Fe II+Si II+S II four-ion spectrum above 5000 Å, proving that in the W7 model, the other metallic lines have a secondary importance in transferring flux compared to Fe III and Fe II lines.

Faint SNe Ia are expected to be redder because of a larger proportion of Fe II (as compared to Fe III) and not because the underlying naïve blackbody is colder. That is, accepting that the primary variation for the peak luminosity is due to nickel mass (Nugent et al. 1995), dimmer supernovae are redder because the underlying ionization stage is primarily Fe II. Figure 7 clearly displays this brighter-bluer evolution for each epoch we simulated.

While the variation with epoch is beyond the scope of this work, the variation with luminosity in part mimics the variation with epoch to some extent. Moreover, the spectra at 10 days after explosion are much bluer than the later ones, because the supernova is much denser and hotter at this epoch, leading to a higher degree of ionisation of the iron core.

This Fe III-Fe II effect on flux transfer agrees with the analysis of Kasen (2006), which explains the second red bump in SNe Ia light curves by the change in opacity due to the recombination of Fe III into Fe II: when the temperature decrease in the SNe Ia envelope is enough for Fe III to recombine into Fe II more flux is transferred from the blue into the red, causing the second red bump.

5.1. Silicon and Sulfur lines

Fig. 12 (top panel) displays Fe II+Fe III two-ion spectrum and Si II single ion spectrum. Si II lines form in the line forming region, contributing little to the global flux transfer but adding lots of structure to the spectrum. As previously mentioned, the ~ 6100 Å trough as well as the Si II $\lambda 6355$ emission peak are dominated by a strong Si II line. The Si II $\lambda 5972$ line is also seen to dominate the second "P-Cygni" trough, but Si II alone fails to account for the blue edge at ~ 5600 Å. We already ruled out Ti II, and the Fe II 5170 Å peak is too blue to account for this edge. Fig. 12 (bottom panel) displays the S II single ion spectrum in addition to the previous ones, showing that S II lines can account for the bluer edge of the $\Re_{Si}$ wavelength region.

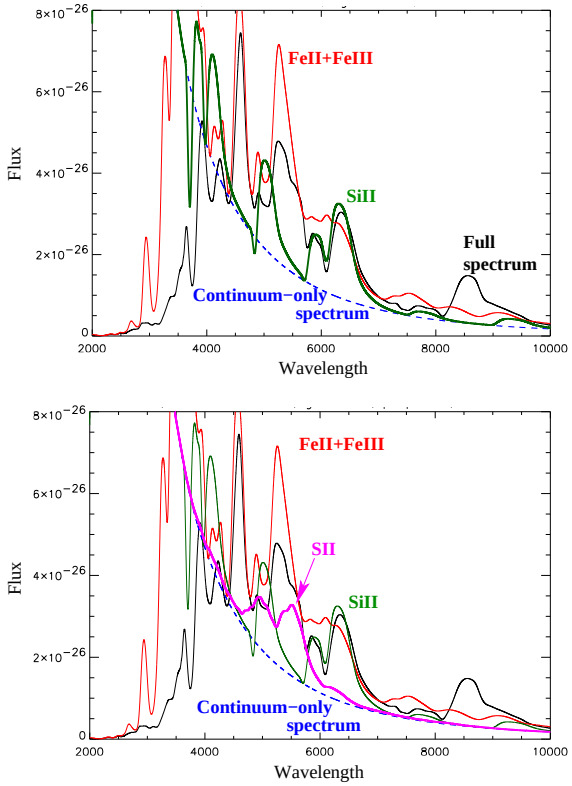

Fig. 12.— Single ion spectra for our faintest luminosity 20 days after explosion. The top panel shows spectra without S II, the bottom panel includes S II. They show that Si II lines alone can not account for the $\Re_{Si}$ wavelength region shape. Fe II and Fe III contribute with their weak lines to the "pseudo-continuum". The blue edge (<5600 Å) of the $\Re_{Si}$ region is dominated by S II lines.

The Si II+S II spectrum of Fig. 13 (top panel) shows that the relative strengths of the peaks and depths due to Si II and S II in the $\Re_{Si}$ wavelength region are consistent with the spectrum of the full W7 model. In Fig. 13 (bottom panel), where all the spectra are rescaled to have the same total flux, if the $\Re_{Si}$ line features are dominated by Si II and S II, it is the Fe III and Fe II lines that provide the flux background. The Fe III+Fe II+Si II+S II spectrum shows that between 5000 Å and 8000 Å the spectrum of the full W7 model is well reproduced by these 4 ions alone. This is an important result for the understanding of the theoretical explanation of the correlation between the line ratios and the absolute B magnitude. Since we have shown that the $\Re_{Si}$ ratio, that is the flux in this wavelength range, depends only on the iron, silicon, and sulfur; to correctly model the line ratio, one must only have a model that correctly accounts for these ions. Clearly we are not there yet, but this result significantly reduces the parameter space that must be studied to obtain physical understanding.

However, we must be cautious due to the fact that our models do not reproduce the observed spectra. For example, W7 does not reproduce the shape of the Si II 6100Å feature (Baron et al. 2006) and thus we could be missing at least one important species in our calculations. Turning this around shows that obtaining the correct variation of $\Re_{SiS}$ with luminosity could be an important filter for obtaining physically correct models.

Similarly, the strong iron features around 4500 Å and 5170 Å are unrealistically large compared to observed spectra. These strong features are a finer probe of a model quality than the overall shape of the spectrum: the thick blend of lines of the iron core is much less sensitive to an abundance variation than the strong lines, forming where the iron blanket has become optically thin.

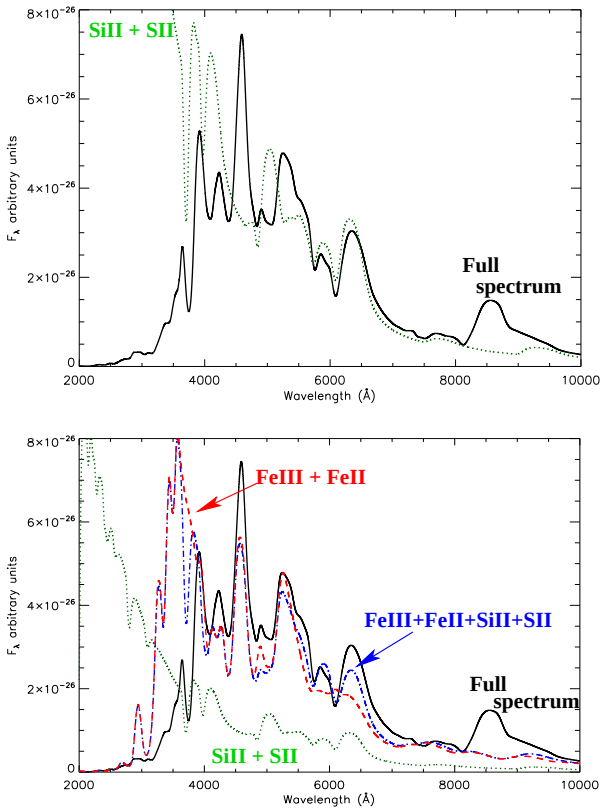

Fig. 13.— Si II+S II two-ion day 20 spectra (top panel, not rescaled, bottom panel, rescaled)

6. $\Re_{SiS}$: observational support of the "multi-layered spectral formation"

6.1. $\Re_{SiS}$ predicted trend: a hotter PHOENIX spectrum

We defined a line ratio $\Re_{SiS}$ (Bongard et al. 2006) as

$$\Re_{SiSS} = \frac{\int_{5500}^{5700} F_\lambda d\lambda}{\int_{6450}^{6200} F_\lambda d\lambda}. \quad (3)$$

We showed that it was better correlated to luminosity than $\Re_{Si}$, and deferred the motivation to the present paper. Here is where we address this question.

As shown in the previous sections, the $\Re_{Si}$ wavelength region is dominated by Fe III, Fe II, Si II, and S II lines. Moreover, for luminosities corresponding to "normal" SNe Ia, the bluer edge of this wavelength region is dominated by S II, since the envelope is still too hot to allow the strong Fe II 5170 Å feature to dominate. As the luminosity decreases, the strength of the Fe II 5170 Å feature increases, this behavior is illustrated in Fig. 14. This effect will have differing importance for the two different definitions of the line ratio, $\Re_{Si}$ and $\Re_{SiS}$. $\Re_{Si}$ will hardly be affected since the depth of the blue Si II feature does not vary significantly; however, $\Re_{SiS}$ uses just this wavelength region and will thus be strongly impacted by the growth of the Fe II λ5170 line.

The "multi-layered line formation" picture shows that the depth of the troughs are not the pertinent quantities to probe the temperature sequence, since the "absorption" features are formed by a complex blend of absorptions and emissions due to ions spanning a wide range of depth. The intermediate $\sim$ 5900 Å $\Re_{Si}$ peak has the same problem, as it is a blend of Fe III, Fe II, and Si II lines. A direct corollary is that $\Re_{Si}$ does not measure line strength evolution as is commonly believed.

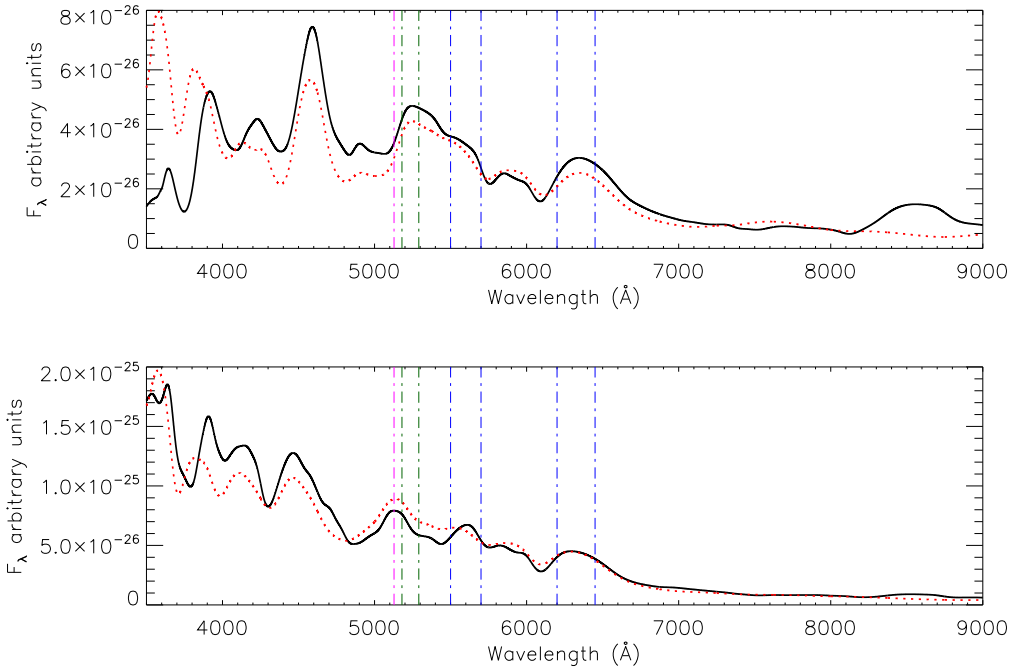

Fig. 14.— The full synthetic day 20 spectrum (solid line) is compared to the day 20 four-ion spectra including Fe III, Fe II, Si II, and S II (dotted line). The top panel shows $M_{bol} = -18.0$, the bottom panel $M_{bol} = -19.0$. The pink vertical line indicates Fe III 5128 Å feature, while the green vertical region shows Fe II strong feature $5170 - 5291$ Å that dominates at lower luminosities. The blue vertical zones are zones where $\Re_{SiS}$ is defined.

The motivation for the definition of $\Re_{SiS}$ was to isolate contributions from Si II and S II lines forming in the same physical region between 10000 km s^{-1} and 15000 km s^{-1}.

There are at least two options for the correlation of $\Re_{SiS}$ with absolute blue magnitude: the silicon and sulfur lines form in the same physical region and their strength is simply determined by the local conditions, or more likely $\Re_{SiS}$ does not measure the region where silicon and sulfur lines form, but rather the conditions where the iron "pseudo-continuum" forms.

Keeping in mind that one should be careful when interpreting single ion spectra, Fig. 9 supports this latter explanation. Fig. 9 (top panel) shows that the Fe II and Fe III blend varies little in the 6100 Å wavelength zone used to compute $\Re_{SiS}$. The consistency in the Si II+S II two-ion spectra shape displayed in Fig. 9 (bottom panel) suggests a small variation of the relative strength of the Si II and S II features. We therefore favor the hypothesis that $\Re_{SiS}$ traces the evolution in shape of the "pseudo-continuum" dominated by iron lines. As such, it should be better correlated with luminosity, since it probes the deeper layers of the supernova. On the other hand, it will be more sensitive to pollution by lines forming further out, especially strong Fe II lines.

6.2. Synthetic vs observed spectra

Up to now we have used the W7 model as a reasonable physical explosion model of SNe Ia, but we did not try to match with observed spectra. We used the knowledge of the abundance structures and the physical structure obtained by `PHOENIX` to probe the line formation process, considering the W7 model as a theoretical supernova of which we had complete knowledge.

The $\Re_{SiS}$ ratio correlates well with absolute blue magnitude (Bongard et al. 2006). In Fig. 15 we display $\Re_{Si}$ and $\Re_{SiS}$ for our day 20 and day 25 models as well as real SNe Ia data. The calculated $\Re_{Si}$ appears to reproduce the observed data quite well for both days 20 and 25. It follows the "normals" quite well and may even extend to the regime of very low luminosity SNe Ia such as SN 1991bg. At first glance, it would appear that the calculated $\Re_{SiS}$ fails to match the observations; however, if one restricts one's attention to the "normals", [Fig. 15 (bottom panel)], in fact the agreement between $\Re_{SiS}$ (for day 25) and the data is better than that for $\Re_{Si}$. The change in slope we observe around $M_B = -19.1$ for day 25 comes from the strong Fe II 5170 Å feature that dominates over S II at lower luminosities.

It should be noted that the W7 model is not expected to reproduce SNe Ia light curves, and certainly cannot be expected to match the observed diversity from fast to slow decliners.

Therefore, the time since explosion should be considered only as indicative, and related only with great care to real supernovæ epochs.

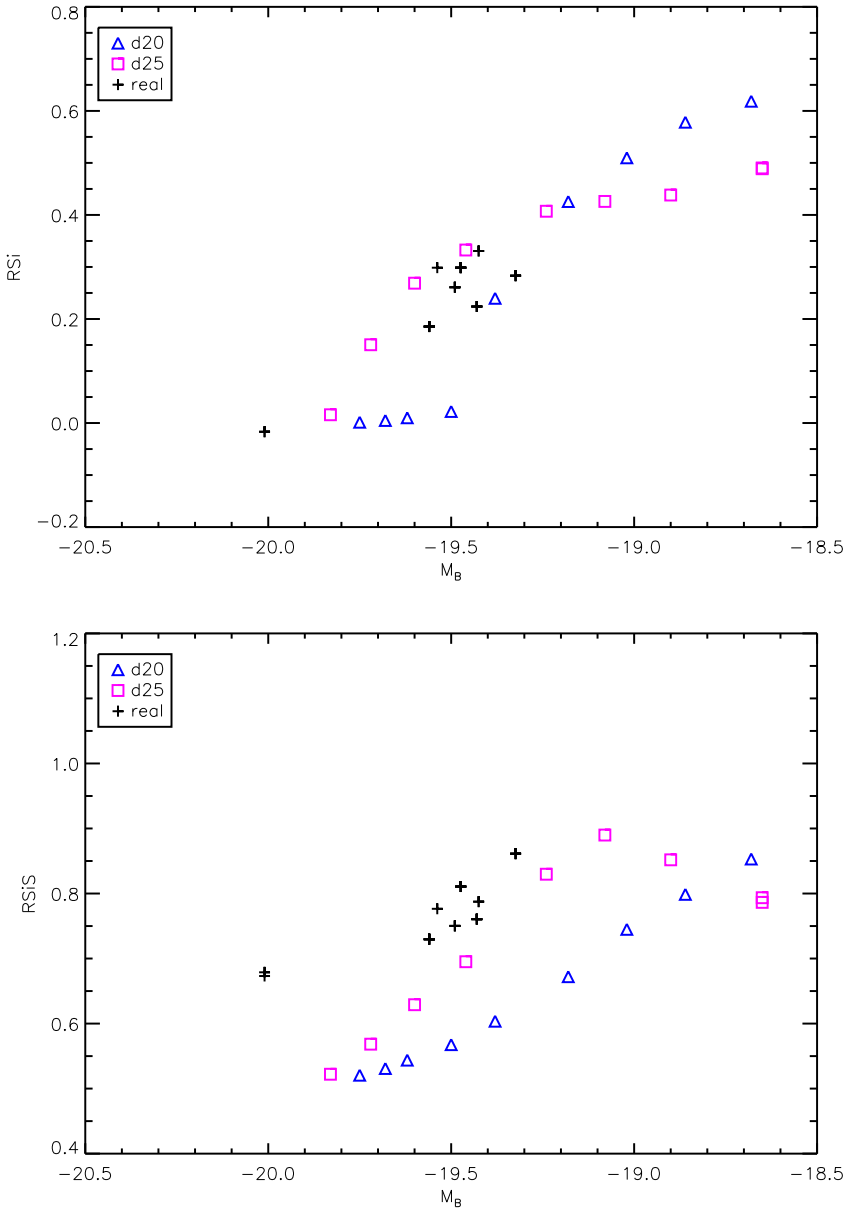

Fig. 15.— $\Re_{Si}$ vs M_B (top panel) and $\Re_{SiS}$ vs M_B (bottom panel) The real data are displayed for reference, and are discussed thoroughly in Bongard et al. (2006). The trends of real and synthetic spectra for 20 and 25 days after maximum are similar. The change in slope between day 20 and day 25 days after explosion is due to Fe II lines starting to dominate the $\Re_{Si}$ wavelength region.

7. Conclusion

We used a grid of LTE PHOENIX synthetic spectra using the W7 model, to study the spectral formation in SNe Ia around the time of maximum light. Instead of focusing on fitting synthetic to observed spectra, we probed the detailed line formation in the synthetic spectrum to try to understand which ion was responsible for which feature, while taking detailed line blending into account.

We analyzed the synthetic spectra in detail to study the line formation in the $\Re_{Si}$ wavelength region, showing that the λ6355 peak and the 6100 Å trough were dominated by Si II lines forming over a blend of Fe II/Fe III lines. The intermediate 5800 Å peak has been shown to be a complex blend of Si II λ6355, Si II λ5972, Fe III, and Fe II weak lines. The Ti II contribution to the 5500 Å trough has been ruled out. We showed that the redder edge was dominated by the λ5972 Si II line whereas the bluer one was dominated by Si II 5455 Å line or Fe II 5170 Å depending on luminosity. Based on our unraveling of the line formation in this wavelength region, we are able to illustrate our motivation for the definition of $\Re_{SiS}$, isolating the Si II and S II contributions of the $\Re_{Si}$ region.

We described a multi-layer model where the observed pseudo-continuum is formed throughout the entire supernova and thus strong features from multiple ionization stages can occur in the observed spectrum. We stress the importance of the numerous weak iron lines and show that their blends dominate the flux transfer. As a corollary, in the multi-layer model, the inner spectrum is not close to a Planck function but contains much more structure background. We showed that the ionization stage of the iron core dominates the SN Ia colors, explaining the brighter-bluer relation at maximum light. Even though a detailed study of time evolution is beyond the scope of this paper, we showed that our results where also qualitatively consistent in this regard, our earlier spectra being systematically much bluer than our later ones.

We thank the anonymous referee for comments which significantly improved the organization of this paper. This work was supported in part by by NASA grants NAG5-3505 and NAG5-12127, NSF grants AST-0307323, AST-0506028, and AST-0707704, and US DOE Grant DE-FG02-07ER41517. S. Bongard and E. Baron acknowledge support from the US Department of Energy Scientific Discovery through Advanced Computing program under contract DE-FG02-06ER06-04. This research used resources of the National Energy Research Scientific Computing Center (NERSC), which is supported by the Office of Science of the U.S. Department of Energy under Contract No. DE-AC02-05CH11231; and the Höchstleistungs Rechenzentrum Nord (HLRN). We thank all these institutions for a generous allocation of computer time.

REFERENCES

Baron, E., Bongard, S., Branch, D., & Hauschildt, P. 2006, ApJ, 645, 480

Baron, E., Branch, D., Hauschildt, P. H., Filippenko, A. V., & Kirshner, R. P. 1999, ApJ, 527, 739

Baron, E. & Hauschildt, P. H. 1998, ApJ, 495, 370

Benetti, S., Cappellaro, E., Mazzali, P. A., Turatto, M., Altavilla, G., Bufano, F., Elias-Rosa, N., Kotak, R., Pignata, G., Salvo, M., & Stanishev, V. 2005, ApJ, 623, 1011

Bongard, S., Baron, E., Smadja, G., Branch, D., & Hauschildt, P. 2006, ApJ, 647, 480

Branch, D., Baron, E., Hall, N., Melakayil, M., & Parrent, J. 2005, PASP, 117, 545

Branch, D., Dang, L. C., Hall, N., Ketchum, W., Melakayil, M., Parrent, J., Troxel, M. A., Casebeer, D., Jeffery, D. J., & Baron, E. 2006, PASP, 118, 560

Fisher, A. 2000, PhD thesis, Univ. of Oklahoma, unpublished

Garnavich, P. M. et al. 2004, ApJ, 613, 1120

Hachinger, S., Mazzali, P. A., & Benetti, S. 2006, MNRAS, 370, 299

Hatano, K., Branch, D., Fisher, A., Deaton, J., & Baron, E. 1999, ApJS, 121, 233

Hatano, K., Branch, D., Lentz, E., Baron, E., Filippenko, A. V., & Garnavich, P. 2000, ApJ, 543, L49

Hauschildt, P. H. & Baron, E. 1999, J. Comp. Applied Math., 109, 41

Hauschildt, P. H., Baron, E., & Allard, F. 1997a, ApJ, 483, 390

Hauschildt, P. H., Baron, E., Starrfield, S., & Allard, F. 1996, ApJ, 462, 386

Hauschildt, P. H., Schwarz, G., Baron, E., Starrfield, S., Shore, S., & Allard, F. 1997b, ApJ, 490, 803

James, J. B., Davis, T. M., Schmidt, B. P., & Kim, A. G. 2006, MNRAS, 370, 933

Kasen, D. 2006, ApJ, 649, 939

Mazzali, P. A. & Podsiadlowski, P. 2006, MNRAS, L32+

Nomoto, K., Thielemann, F.-K., & Yokoi, K. 1984, ApJ, 286, 644

Nugent, P., Phillips, M., Baron, E., Branch, D., & Hauschildt, P. 1995, ApJ, 455, L147

Stehle, M., Mazzali, P., Benetti, S., & Hillebrandt, W. 2005, MNRAS, 360, 1231